Springtime phytoplankton responses to light and iron availability along the western Antarctic Peninsula

Joy-Warren, Hannah L.; Alderkamp, Anne Carlijn; van Dijken, Gert L.; J. Jabre, Loay; Bertrand, Erin M.; Baldonado, Evan N.; Glickman, Molly W.; Lewis, Kate M.; Middag, Rob; Seyitmuhammedov, Kyyas

Published in:
Limnology and Oceanography

DOI:
10.1002/lno.12035

LIMNOLOGY and OCEANOGRAPHY

ASLO

Limnol. Oceanogr. 67, 2022, 800–815

doi: 10.1002/lno.12035

Springtime phytoplankton responses to light and iron availability along the western Antarctic Peninsula

Hannah L. Joy-Warren,[1*,a] **Anne-Carlijn Alderkamp**,[1,b] **Gert L. van Dijken**,[1] **Loay J. Jabre**,[2] **Erin M. Bertrand**,[2] **Evan N. Baldonado**,[1] **Molly W. Glickman**,[1] **Kate M. Lewis**,[1] **Rob Middag**,[3,4] **Kyyas Seyitmuhammedov**,[4,c] **Kate E. Lowry**,[1,5] **Willem van de Poll**,[6] **Kevin R. Arrigo**[1]

[1]Department of Earth System Science, Stanford University, Stanford, California
[2]Department of Biology, Dalhousie University, Halifax, Nova Scotia, Canada
[3]Department of Ocean Systems (OCS), NIOZ Royal Netherlands Institute for Sea Research, Texel, The Netherlands
[4]Department of Chemistry, University of Otago, Dunedin, New Zealand
[5]Department of Biology, Woods Hole Oceanographic Institution, Woods Hole, Massachusetts
[6]Department of Ocean Ecosystems, Energy and Sustainability Research Institute Groningen, University of Groningen, Groningen, The Netherlands

Abstract

Light and iron availability are intertwined in controlling Southern Ocean primary production because several photosynthetic proteins require iron. Changes in light and iron availability can also affect phytoplankton species composition, which impacts nutrient cycling, carbon drawdown, and food web structure. To investigate the interactive effects of light and iron on phytoplankton growth, photosynthesis, photoacclimation strategy, micronutrient stress-induced protein expression, and species composition, we conducted five bioassay experiments during spring in waters along the western Antarctic Peninsula with four treatments: low light (LL) or high light (HL) combined with or without iron addition. This region has rarely been studied in spring. We found that light limits growth while iron does not, despite overall low iron concentrations. Our results demonstrate that phytoplankton were LL acclimated in situ but photosynthetically optimized for higher light than they were experiencing, likely due to a highly dynamic light regime. Expression patterns of micronutrient stress-induced proteins were consistent with iron stress in off-shelf regions, but remarkably this iron stress did not result in lower carbon fixation and growth rates. Notably, manganese drawdown was highest under elevated light, suggesting a possible role in managing HL, although high flavodoxin expression indicated that *Phaeocystis antarctica* may not have been manganese-limited. Although light and iron treatments did not impact species composition, high methionine synthase indicated that diatoms could have experienced stress induced by low vitamin B_{12}, potentially contributing to *P. antarctica*'s general dominance throughout the experiments. Our results indicate that *P. antarctica* may be better adapted to spring conditions than diatoms.

Light and iron (Fe) availability are the dominant factors controlling Southern Ocean primary production (Martin et al. 1990; Sunda and Huntsman 1997; Boyd et al. 2012). Phytoplankton Fe requirements are intertwined with light availability because some photosynthetic proteins require Fe (Eberhard et al. 2008). Phytoplankton respond to changes in light through photoacclimation, in part by upregulating photoprotective pigments in high light (HL) or

*Correspondence: hjoyw@uw.edu

Additional Supporting Information may be found in the online version of this article.

[a]Present address: Cooperative Institute for Climate, Ocean, and Ecosystem Studies (CICOES), University of Washington, Seattle, Washington, USA
[b]Present address: Biology Department, Foothill College, Los Altos Hills, California, USA
[c]Present address: Department of Chemistry, Norwegian University of Science and Technology (NTNU), P.O. Box 8900, 7491, Trondheim, Norway

Author Contribution Statement: H.J.-W.: took measurements from experiments; analyzed phytoplankton growth, biomass, photosynthesis, photoacclimation, and species composition data; integrated all datasets and analysis; wrote all sections except proteomics and parts of trace metals; edited manuscript. A.-C.A., G.L.v.D.: experimental design; conducted experiments and took measurements; edited manuscript. L.J.J.: developed methods, analyzed, and wrote proteomics sections; edited manuscript. E.M.B.: conducted experiments and took measurements; developed methods, analyzed, and wrote proteomics sections; edited manuscript. E.N.B., M.W.G.: analyzed species composition data. K.M.L.: took measurements from experiments; edited manuscript. R.M.: conducted experiments and took measurements; analyzed and wrote trace metals section; edited manuscript. K.S.: analyzed trace metals; edited manuscript. K.E.L.: conducted experiments and took measurements; edited manuscript. W.v.d.P.: analyzed HPLC/CHEMTAX data; edited manuscript. K.R.A.: experimental design; data analysis support; edited manuscript.

photosynthetic pigments in low light (LL) (MacIntyre et al. 2000). Cellular Fe requirements generally increase in LL as cells upregulate synthesis of Fe-containing photosynthetic proteins (Sunda and Huntsman 1997). However, Southern Ocean phytoplankton may have adapted to perpetually low Fe conditions by increasing their antenna size (no additional Fe required) to capture more photons instead of increasing the number of photosynthetic reaction centers (Strzepek et al. 2012; Alderkamp et al. 2019). Phytoplankton can also reduce Fe demand by substituting Fe-containing photosynthetic proteins with non-Fe containing analogs (LaRoche et al. 1996; Peers and Price 2006; Bender et al. 2018).

Both light and dissolved Fe follow strong seasonal cycles in the Southern Ocean. With spring, full darkness gives way to continuous daylight as melting sea ice permits both illumination of the surface ocean and stratification, concentrating phytoplankton in the newly lit underwater environment. In general, the Southern Ocean is Fe deplete, and thus phytoplankton production is often limited by low dissolved Fe availability (Martin et al. 1990). Fe is replenished during the winter from deep-water mixing and resuspension from sediments in coastal regions, continuing into the spring through glacial melt, sea ice melt, and precipitation (Annett et al. 2015, 2017). The available Fe is quickly consumed by phytoplankton in the spring, leading to extremely low surface water dissolved Fe concentrations in summer (Annett et al. 2017).

Fe requirements are also species-specific (Strzepek et al. 2011). In the Southern Ocean, the dominant phytoplankton taxa are *Phaeocystis antarctica* and diatoms (Arrigo et al. 1999). *P. antarctica* has higher Fe : carbon (C) uptake rates than Southern Ocean diatoms (Zhu et al. 2016) and cellular Fe : C ratios (volume normalized) that are about two times greater than those of large Southern Ocean diatoms (Strzepek et al. 2011). However, diatoms are Fe-limited at higher Fe concentrations than *P. antarctica* (Trimborn et al. 2019). In laboratory experiments, Southern Ocean diatoms and *P. antarctica* responded differently to light and Fe limitation, with *P. antarctica* achieving higher growth rates than diatoms across light and Fe conditions (Strzepek et al. 2011; Strzepek et al. 2012; Trimborn et al. 2019). Both groups acclimate to irradiance in low Fe conditions by increasing the size of their antennae rather than the number of photosynthetic units; however, Southern Ocean diatoms have even larger antennae and fewer reaction centers than *P. antarctica* (Strzepek et al. 2012; Strzepek et al. 2019; Trimborn et al. 2019). In addition to Fe and light, the availability of manganese (Mn) (Middag et al. 2013; Wu et al. 2019) and vitamin B_{12} (Bertrand et al. 2007) can be colimiting factors of Southern Ocean primary production, and likely help shape species composition.

Summertime controls on phytoplankton production in waters along the western Antarctic Peninsula have been well documented (Ducklow et al. 2007); however, little work has been done in this region during the highly productive spring. Understanding the factors that control springtime phytoplankton production will fill a critical gap in our knowledge of the seasonal transition in phytoplankton populations from winter to summer. Therefore, we conducted a series of bioassay experiments in waters along the western Antarctic Peninsula to investigate the interactive effects of light and Fe on phytoplankton populations.

The waters along the western Antarctic Peninsula are seasonally ice-covered and home to a highly productive ecosystem (Ducklow et al. 2007). Both diatoms and *P. antarctica* are present in spring (Annett et al. 2010; Arrigo et al. 2017) and there is some evidence that *P. antarctica* dominates the phytoplankton community in spring (Annett et al. 2010; Arrigo et al. 2017; Van Leeuwe et al. 2020) when deep mixed layers and ice cover create low but variable light (Arrigo et al. 1999; Joy-Warren et al. 2019). Summer diatom dominance follows (Trimborn et al. 2017; Van Leeuwe et al. 2020), when melting ice and shoaling mixed layers create high and consistent light in the surface of the ocean (Arrigo et al. 1999). The interplay between light and seasonal nutrient availability (such as Fe, Mn, and vitamin B_{12}) may help explain the seasonal transition from springtime *P. antarctica* dominance to summer diatom dominance, which was demonstrated in model results of the Amundsen Sea (Kwon et al. 2021). This is ecologically important because the two taxa support distinct upper trophic levels (diatoms: krill, penguins, seals, and whales; non-diatoms: salps or a microbial food web; Moline et al. 2004; Murphy et al. 2013; Saba et al. 2014) and contribute disproportionately to carbon drawdown, with *P. antarctica* taking up 56% more carbon dioxide per mole of phosphate than diatoms (Arrigo et al. 1999).

The objective of this work is to determine if light, Fe, or the interaction of light and Fe controls phytoplankton growth, biomass, photosynthesis, photoacclimation strategy, micronutrient stress-induced protein expression, and species composition along the western Antarctic Peninsula during spring, prior to the large summer bloom that can go into Fe-limitation (Annett et al. 2017). To do so, we conducted five bioassay experiments (6 d each), each with two levels of light (high and low) and Fe (with and without Fe addition). Our methods enable novel insights by measuring trace metals (Fe and Mn) and micronutrient stress-induced protein expression in a series of bioassay experiments.

Methods

Bioassay experiments

To investigate how varying light and Fe, and their interaction, impact phytoplankton populations, we conducted bioassay experiments along the western Antarctic Peninsula during the Phantastic II cruise in austral spring from 31 October 2014 to 21 November 2014 (NBP14-09; Fig. 1). We collected seawater from surface depths (10 and 25 m; Table 1; Supporting Information Table S1; *see* Arrigo et al. 2017 for water sampling

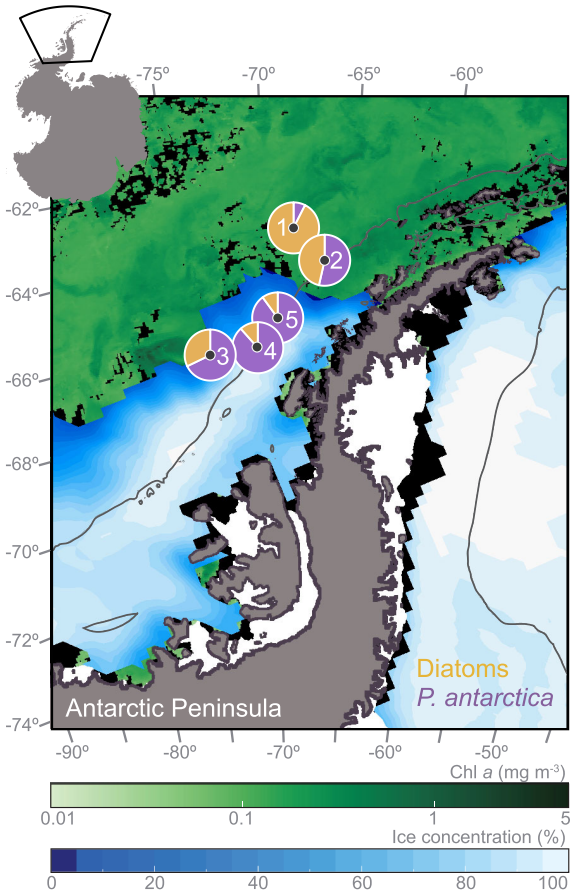

Fig. 1. Experiment numbers and locations (black dots) and initial species composition (pie charts; diatoms: yellow, *Phaeocystis antarctica*: purple). SSM/I satellite ice concentration (15 November 2014) and monthly MODIS/Aqua Chl *a* (November 2014). Gray line: 1000 m contour. The region shown is indicated by a black box on the inset map of Antarctica.

methods) using trace metal clean methods, which were used throughout the experiments (*see* Gerringa et al. 2015 for details). Our conductivity-temperature-depth system was equipped with a Biospherical/Licor photosynthetically active radiation (PAR) irradiance sensor

Unfiltered seawater was incubated on deck at in situ water temperature in acid-washed 2 L polycarbonate bottles under HL and LL. HL received 30% of surface PAR, representing 0–10 m within the respective water columns from which each experiment was initiated. LL treatments received 3% of surface PAR, representing 10–43 m. Light levels were achieved by shading transparent incubators with neutral density mesh screening. Each light level had triplicate Fe-amended (4 nmol L^{-1} dissolved Fe aadded to each bottle) and unamended treatments, resulting in four treatments: LL without added Fe (LL *no added* Fe), HL without added Fe (HL *no added* Fe), LL with added Fe (LL + Fe), and HL with added Fe (HL + Fe). Both dissolved Fe and Mn were monitored throughout the experiments.

Full bottles were sampled for nutrients and physiology on Days 4 and 6 (results are discussed for Day 6 when macronutrients and dissolved Fe were not exhausted) and protein measurements (Day 4 only to minimize bottle effects on protein expression changes). All parameters were measured in triplicate, except for carbon fixation parameters, which were measured on a pooled sample from the triplicates.

Dissolved nutrients

To calculate nutrient uptake by phytoplankton and monitor for nutrient limitation during experiments, nitrate (NO_3^-), phosphate (PO_4^{3-}), and silicate ($Si(OH)_4$) were sampled in the experiments, as detailed in Arrigo et al. (2017). In brief, samples were collected by filtering seawater through a 0.2 μm syringe filter and stored in the dark at −20°C (NO_3^- and PO_4^{3-}) or 4°C ($Si(OH)_4$) to prevent precipitation. Samples were analyzed on a Bran and Luebbe trAAcs 800 Gas-Segmented Continuous Flow Analyzer, as in Gerringa et al. (2019).

Trace metals

Dissolved Fe and Mn concentrations used to calculate drawdown during experiments were analyzed after preconcentration with a seaFAST system using a Thermo Element2 sector-field inductively coupled plasma mass spectrometer under cleanroom laboratory conditions based on a multielement method using Nobias PA1 as a chelating resin (Gerringa et al. 2020). Drawdown of dissolved Fe and Mn was calculated by subtracting the concentration observed on Day 6 from the starting concentration, assuming a starting concentration of 2 nM for +Fe treatments (based on 50% of added dissolved Fe adsorbed onto experiment bottle wall, as suggested by Fisher et al. 2007; *see* Results: Trace Metals).

Physiological measurements

Pigments and biomass

Phytoplankton biomass in the experiments was assessed by measuring pigment concentrations and particulate organic carbon and nitrogen (POC and PON). Samples were collected by filtration under low vacuum pressure (< 5 mm Hg) through 25 mm Whatman glass-fiber filters (GF/F, nominal pore size 0.7 μm).

Samples for pigment analysis were filtered under LL, snap frozen in liquid nitrogen, stored at −80°C, and analyzed following the extraction method of Van Leeuwe et al. (2006) and the high-performance liquid chromatography method of Van Heukelem and Thomas (2001). Pigment concentrations were compared by normalizing to chlorophyll *a* (Chl *a*) and grouped into photosynthetic accessory pigments (PSP = Chl *a* + Chl *b* + Chl c_2 + Chl c_3 + 19′-butanoyloxyfucoxanthin + 19′-hexanoyloxyfucoxanthin + 19′-hexanoyloxy-4-ketofucoxanthin + fucoxanthin + peridinin + prasinoxanthin) and photoprotective pigments (PPP = diadinoxanthin [DD] + diatoxanthin [DT] + violaxanthin + zeaxanthin + lutein + β-carotene) (Higgins et al. 2011; Van Leeuwe et al. 2014; Arrigo et al. 2017).

Table 1. Conditions at stations where bioassay experiments were initiated and light levels during experiments. Mixed layer PAR is the mean photosynthetically active radiation in the mixed layer. Low light and high light are the mean PAR that samples experienced during incubation. Nutrients (nitrate: NO_3^-, phosphate: PO_4^{3-}, silicate: $Si(OH)_4$; mean ± 1 standard deviation for dissolved iron (Fe) and dissolved manganese (Mn)) and biological parameters (Chl *a*, mean ± 1 standard deviation for *Phaeocystis antarctica* and diatoms [subdivided into centric and pennate diatoms]) are reported for the sampling depth (10 m for Experiments 1 and 2; 25 m for Experiments 3–5).

	Experiment 1	Experiment 2	Experiment 3	Experiment 4	Experiment 5
Parameter	**Station 4**	**Station 10**	**Station 50**	**Station 67**	**Station 78**
Mixed layer PAR (μmol photons m^{-2} s^{-1})	29.5	23.7	58.4	4.2	31.0
Low light incubation (μmol photons m^{-2} s^{-1})	14.3	15.1	23.0	17.5	13.5
High light incubation (μmol photons m^{-2} s^{-1})	143	151	230	175	135
NO_3^- (μmol L^{-1})	28.43	27.20	27.41	29.48	28.83
PO_4^{3-} (μmol L^{-1})	1.86	1.85	1.82	2.01	1.93
$Si(OH)_4$ (μmol L^{-1})	30.5	46.0	—	64.7	52.1
Dissolved Fe (nmol L^{-1})	0.09 ± 0.01	0.14 ± 0.01	0.27 ± 0.03	0.69 ± 0.07	0.14 ± 0.01
Dissolved Mn (nmol L^{-1})	0.16 ± 0.01	0.18 ± 0.01	0.17 ± 0.01	1.15 ± 0.02	0.39 ± 0.01
Chl *a* (mg m^{-3})	0.33	1.44	1.54	0.21	0.32
P. antarctica (%)	7.5 ± 11	54 ± 21	68	88	90
Diatoms (%)	93 ± 11	46 ± 21	32	12	10
Centric diatoms (%)	90 ± 10	45 ± 21	32	9.1	8.6
Pennate diatoms (%)	2.9 ± 0.4	1.2 ± 0.2	0.2	2.5	1.4

Samples for POC and PON were filtered onto precombusted (450°C for 4 h) GF/F filters, which were dried (60°C for 24 h) and stored at room temperature until analysis on a Costech Elemental Analyzer using acetanilide as a calibration standard.

Species composition

To identify initial species composition and any possible species composition shifts throughout experiments, phytoplankton species composition was assessed visually using a FlowCam (VS IVc, Fluid Imaging Technologies) as described in Joy-Warren et al. (2019) and detailed in Supporting Information Section S1.

Variable fluorescence

Phytoplankton photophysiological status was monitored by measuring variable fluorescence using a FIRe fluorometer (Fluorescence Induction and Relaxation System; Satlantic LP), blanked with 0.2 μm filtered seawater from the same station. Samples were dark-acclimated on ice for 30 min to fully oxidize the photosynthetic reaction centers prior to measuring the maximum photochemical efficiency of photosystem II (PSII) (F_v/F_m) and functional absorption cross section of PSII (σ_{PSII}; $Å^2$ $photon^{-1}$) (Gorbunov et al. 1999).

Phytoplankton carbon fixation characteristics

Photosynthesis-Irradiance curves were used to determine maximum biomass-specific photosynthetic rates (P^*_{max}; mg C mg^{-1} Chl *a* h^{-1}), light-limited rates of photosynthesis (α*; mg C mg^{-1} Chl *a* h^{-1} [μmol photons m^{-2} s^{-1}]$^{-1}$), and photoacclimation parameters (E_k; μmol photons m^{-2} s^{-1}) using methods described in Arrigo et al. (2010) (*see* Supporting Information Section S2).

Absorption and quantum yield

Phytoplankton photophysiological status was characterized with particulate absorption (a_p), absorption by phytoplankton (a_{ph}), the spectrally averaged Chl *a*-specific coefficient for phytoplankton ($\bar{a}^*$), and the maximum quantum yield of photosynthesis (ϕ_m), which were calculated as described in Lewis et al. (2018).

Phytoplankton growth rates

To quantify phytoplankton growth during the experiments, growth rates (μ) were estimated from measurements of mean POC at the beginning and end of each incubation and assume exponential growth:

$$\mu = \frac{\ln\left(\frac{POC_{Day\ 6}}{POC_{Day\ 0}}\right)}{6\,d},$$

assuming that changes in POC over time reflect increases in phytoplankton biomass.

Proteomics

To quantify micronutrient stress-induced changes in proteins, protein samples were collected on 0.22 μm Sterivex™ filters via peristaltic pumping and stored at −80°C until analysis. Targeted protein measurements were conducted following methods described in Wu et al. (2019). For details, *see* Supporting Information Section S3.

Sea ice

We characterized sea ice in the sampling region using daily sea ice concentration images from the Special Sensor Microwave Imager/Sounder (25 km resolution, NASA Team algorithm; National Snow and Ice Data Center, https://nsidc.org).

Statistical analysis

Treatment and interactive effects were assessed using the Aligned Rank Transform test, which transforms nonparametric factorial data such that ANOVA can be used (Wobbrock et al. 2011). Because results were generally consistent across experiments (*see* Supporting Information Figs. S1, S2; Tables S2, S3) and sample sizes for each treatment within experiments were small ($n = 3$), we combined the data from all five experiments to analyze the treatment effects ($n = 15$). To normalize variables across experiments, tests were performed on the fractional change for each variable from Days 0 to 6 (i.e., [Day 6 – Day 0]/Day 0) of the experiment (individual values are presented in Supporting Information Tables S4 and S5).

Variables impacting dissolved Mn drawdown were assessed using linear regressions (lm function) in the statistical software package R, following the formula: $y = \beta_1 x + \beta_0$.

p-values are given for the Aligned Rank Transform tests and linear regressions and likely differences among treatments are discussed at $p < 0.1$. *p*-values between 0.05 and 0.1 are discussed as possible effects. We interpret $p > 0.1$ as giving no evidence against the hypothesis that the treatment effects have the same mean, either indicating that there is no true effect or that the variance obscured the effect.

Results

Initial experimental conditions

Experiments 1, 2, 3, and 5 were initiated off the continental shelf in the region between the Southern Antarctic Circumpolar Current Front and the Southern Boundary of the Antarctic Circumpolar Current. Experiment 4 was initiated on the continental shelf, shoreward of the Southern Boundary of the Antarctic Circumpolar Current (Supporting Information Table S1). *See* Supporting Information Section S4 for an overview of our study site and a detailed description of the initial experimental conditions.

Sea ice concentration varied from 24 to 93% (Supporting Information Table S1) and was highest near the shelf break and toward the southern end of our study region (Fig. 1). Mean PAR in the mixed layer (determined as in Joy-Warren et al. 2019) at the time of sampling was low (mean: 29 μmol photons m^{-2} s^{-1}) due to sea ice cover and deep mixed layers, ranging from 4.2 to 58 μmol photons m^{-2} s^{-1}.

Macronutrient (NO_3^-, PO_4^3, and $Si(OH)_4$) concentrations were considerably above growth-limiting levels for phytoplankton (*see* Arrigo et al. 2017) and were not completely consumed in any of the experiments by Day 6. Therefore, we assume that observed changes were due to experimental treatments and not macronutrient limitation. Dissolved Fe ranged between 0.09 and 0.69 nmol L^{-1} and dissolved Mn between 0.16 and 1.15 nmol L^{-1} at sampling depths where experiments were initiated (Table 1).

Day 0 species composition at experimental sites ranged from diatom-dominated (Experiment 1, 93 ± 11% diatoms), to mixed diatoms and *P. antarctica* (Experiment 2, 46 ± 21% diatoms and 54 ± 21% *P. antarctica*), to *P. antarctica*-dominated (Experiments 3, 4, and 5, 68–90% *P. antarctica*; Fig. 1; Table 1; and Supporting Information Fig. S1).

Light and Fe effects on nutrient uptake and phytoplankton growth

Macronutrients

Nutrient drawdown during the experiments varied by light treatment. NO_3^-, PO_4^{3-}, and $Si(OH)_4$ were drawn down more in HL treatments than in LL treatments (NO_3^-: $p = 0.0029$; PO_4^{3-}: $p = 0.0010$; $Si(OH)_4$: $p = 0.097$; Fig. 2; Tables 2, 3). In LL treatments, NO_3^- was drawn down on average by 2.99 ± 1.23 μmol L^{-1} relative to Day 0, while in HL treatments NO_3^- was drawn down on average by 4.98 ± 3.11 μmol L^{-1}. Nutrient drawdown was not different between treatments with and without Fe addition (Supporting Information Fig. S2 and Table S3), and we did not observe an interactive effect between light and Fe on nutrient drawdown.

Trace metals

Both dissolved Fe and Mn were depleted to low values by Day 6 among experiments with low initial dissolved Fe and Mn (Fig. 2; Table 1; Supporting Information Table S2). Drawdown of dissolved Fe and Mn did not vary significantly among treatments across all experiments, except for dissolved Fe drawdown in +Fe treatments (Table 2). Iron addition led to a higher dissolved Fe drawdown than in treatments without Fe addition; however, this is in part due to rapid precipitation and adsorption onto bottle walls. For polycarbonate bottles, Fisher et al. (2007) estimated that ~ 50% of added Fe adsorbs onto the bottle walls and therefore relative differences in dissolved Fe are more important than absolute numbers. Drawdown of dissolved Fe in treatments without Fe addition varied from 0.02 to 0.46 nmol L^{-1} (16–67% relative to starting concentration) and drawdown of dissolved Mn in almost all treatments varied from 0.02 to 0.15 nmol L^{-1} (3–84% relative to starting concentration). In most experiments, HL treatments had a greater dissolved Mn drawdown than LL treatments (Supporting Information Table S3).

Across all experiments, the greatest dissolved Mn drawdown was correlated with the lowest F_v/F_m values ($p = 0.0027$) (Supporting Information Fig. S4a). Dissolved Mn drawdown was also positively correlated to indicators of growth, such as macronutrient consumption (NO_3^-: $p = 0.0018$; PO_4^{3-}: $p < 0.001$), POC accumulation ($p < 0.001$), and growth rate ($p = 0.0061$), and negatively correlated to the ratio of POC to PON

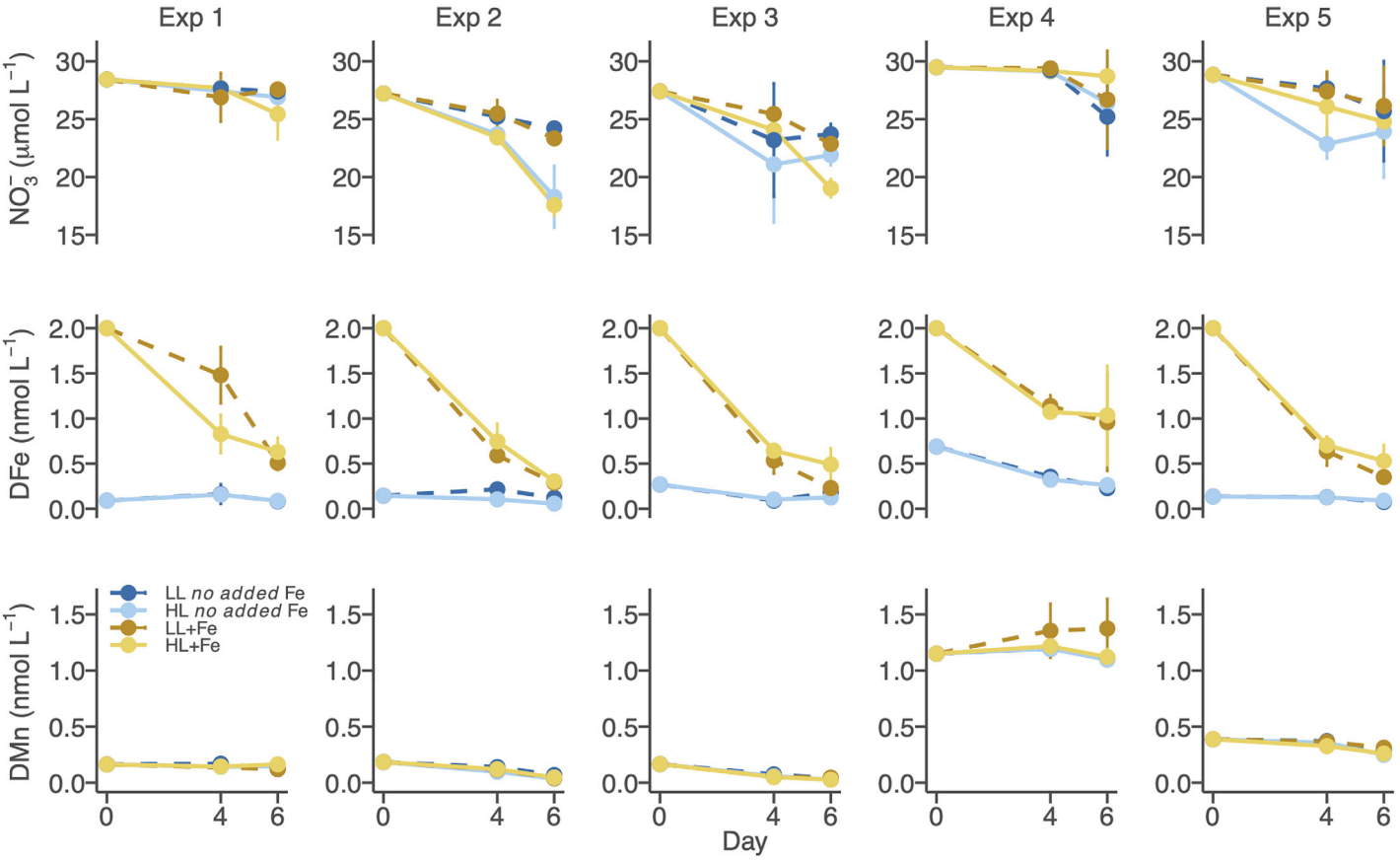

Fig. 2. Concentrations of NO_3^- (nitrate; µmol L^{-1}), DFe (dissolved iron; nmol L^{-1}), and DMn (dissolved manganese; nmol L^{-1}) throughout experiments. Error bars represent 1 standard deviation.

($p < 0.0001$). Dissolved Mn drawdown was greatest when *P. antarctica* made up the largest fraction of the community ($p = 0.0089$).

Biomass

Initial POC concentrations ranged from 45 to 179 mg m^{-3} (mean: 104 ± 64 mg m^{-3}) and initial PON concentrations ranged from 7 to 33 mg m^{-3} (mean: 17.4 ± 11.5 mg m^{-3}; Supporting Information Table S2). POC and PON increased in all treatments relative to Day 0 (POC: 104 ± 64 mg m^{-3}; PON: 17.4 ± 11.5 mg m^{-3}), but increased more in HL treatments (POC: 356 ± 239 mg m^{-3}; PON: 62.0 ± 46.4 mg m^{-3}) than in LL treatments (POC: 265 ± 165 mg m^{-3}; PON: 42.2 ± 28.8 mg m^{-3}; both POC and PON: $p < 0.001$; Fig. 3a; Supporting Information Table S2), consistent with the greater nutrient drawdown in HL treatments. Similarly, POC-based growth rate was higher in HL (0.20 ± 0.05 d^{-1}) than in LL (0.15 ± 0.04 d^{-1}) treatments ($p < 0.001$; Tables 2 and 3).

Initial Chl *a* concentrations ranged from 0.32 to 1.54 mg m^{-3} (mean: 0.79 ± 0.64 mg m^{-3}; Table 1). Chl *a* increased in all treatments relative to Day 0, but increased more in the LL treatments (2.16 ± 1.70 mg m^{-3}) than in HL treatments (1.71 ± 1.27 mg m^{-3}; $p < 0.001$; Fig. 3b), hence the negative relationship between light and Chl *a* (Table 2). Correspondingly, the POC/Chl *a* ratio increased in HL treatments (226 ± 36) relative to Day 0 (171 ± 66) and decreased in LL treatments (143 ± 32) relative to Day 0 (Fig. 3c; Supporting Information Table S2). The POC/PON ratio was greater in LL treatments (7.92 ± 1.26) than in HL treatments (7.29 ± 0.99; $p = 0.065$; Fig. 3d; Supporting Information Table S2).

There was no evidence that Fe addition affected POC, PON, Chl *a*, growth rate, POC/Chl *a*, or POC/PON, nor was there evidence of an interactive effect between light and Fe treatments (Table 2; for individual experiment effects *see* Supporting Information Table S3). The light and Fe effects on phytoplankton growth are described in Supporting Information Section S5.

Light and Fe effects on photosynthetic parameters

F_v/F_m *and* σ_{PSII}

On Day 0, F_v/F_m (0.56 ± 0.06) and σ_{PSII} (588 ± 104 $Å^2$ photon^{-1}) were at their highest values during the experiment (Supporting Information Table S2). By Day 6, F_v/F_m was higher in LL treatments (0.53 ± 0.07) than in HL treatments (0.47 ± 0.08; $p < 0.001$; Fig. 4a; Table 2). In +Fe treatments,

Table 2. Treatment effects (calculated from the fractional change between Day 0 and Day 6) analyzed with Aligned Rank Transform tests. Effects are shown for light treatments (LL vs. HL), Fe treatments (*no added* Fe vs. +Fe), and the interaction between light and Fe. Circles indicate level of significance and (+) indicates a positive relationship while (−) indicates a negative relationship. NO_3^-: nitrate (μmol L^{-1}); PO_4^{3-}: phosphate (μmol L^{-1}); $Si(OH)_4$: silicate (μmol L^{-1}); Fe: iron (nmol L^{-1}); Mn: manganese (nmol L^{-1}); Chl *a*: chlorophyll *a* concentration (mg m^{-3}); $\overline{a}^*$: mean Chl *a*-specific absorption coefficient (m^2 mg^{-1} Chl *a*); POC (PON): particulate organic carbon (nitrogen) (mg m^{-3}); POC-based growth rate (d^{-1}); POC/Chl *a* (g : g); POC/PON (mol : mol); F_v/F_m: maximum photochemical efficiency of photosystem II (unitless); σ_{PSII}: effective absorption cross section of photosystem II ($Å^2$ $photon^{-1}$); P^*_{max}: maximum photosynthetic rate (mg C mg^{-1} Chl *a* h^{-1}); α^*: photosynthetic efficiency (mg C mg^{-1} Chl *a* h^{-1} [μmol photons m^{-2} s^{-1}]$^{-1}$); E_k: photoacclimation parameter (μmol photons m^{-2} s^{-1}); ϕ_m: maximum quantum yield of photosynthesis (mol C mol^{-1} photons absorbed); (DD + DT)/Chl *a*: ratio of diadinoxanthin and diatoxanthin to chlorophyll *a* (unitless); PPP/PSP: ratio of photoprotective pigments to photosynthetic pigment (unitless).

Parameter		Light		Iron		Light × iron
Nutrients	NO_3^-	••	(−)			
	PO_4^{3-}	••	(−)			
	$Si(OH)_4$	○	(−)			
Trace metals	Fe			•••	(+)	
	Mn					
Biomass	Chl *a*	•••	(−)			
	$\overline{a}^*$					
	POC	•••	(+)			
	PON	•••	(+)			
	Growth rate (POC)	•••	(+)			
	POC/Chl *a*	•••	(+)			
	POC/PON	○	(−)			
Variable fluorescence	F_v/F_m	•••	(−)	•••	(+)	
	σ_{PSII}			•••	(−)	
Carbon fixation	P^*_{max}					
	α^*					
	E_k					
	ϕ_m					
Pigments	(DD + DT)/Chl *a*	•••	(+)	•••	(−)	•
	PPP/PSP	•••	(+)			
Species composition	Diatoms					
	Phaeocystis antarctica					

1 > (no symbol) > 0.1 > ○ > 0.05 > • > 0.01 > •• > 0.001 > ••• > 0

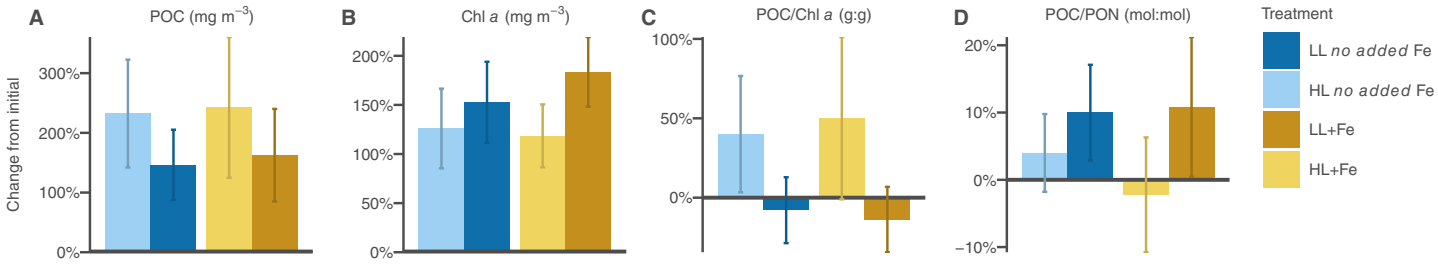

Fig. 3. Photosynthetic response to light treatment (HL, LL) and dissolved Fe (+Fe) additions shown in percent changes from initial averaged across experiments for (**a**) POC: particulate organic carbon (mg m^{-3}), (**b**) Chl *a*: Chlorophyll *a* (mg m^{-3}), (**c**) POC/Chl *a* (g:g), (**d**) POC/PON: POC/particulate organic nitrogen (mol : mol). Bar height represents mean and error bars show 1 standard deviation.

F_v/F_m was also higher, and correspondingly σ_{PSII} was lower (F_v/F_m: 0.53 ± 0.05; σ_{PSII}: 406 ± 51 $Å^2$ $photon^{-1}$), than in the treatments without added Fe (F_v/F_m: 0.47 ± 0.09; σ_{PSII}: 461 ± 69 $Å^2$ $photon^{-1}$; both: $p < 0.001$; Fig. 4b; Table 2). There was neither an effect of light treatment on σ_{PSII} nor an interactive effect between light and Fe on F_v/F_m or σ_{PSII}.

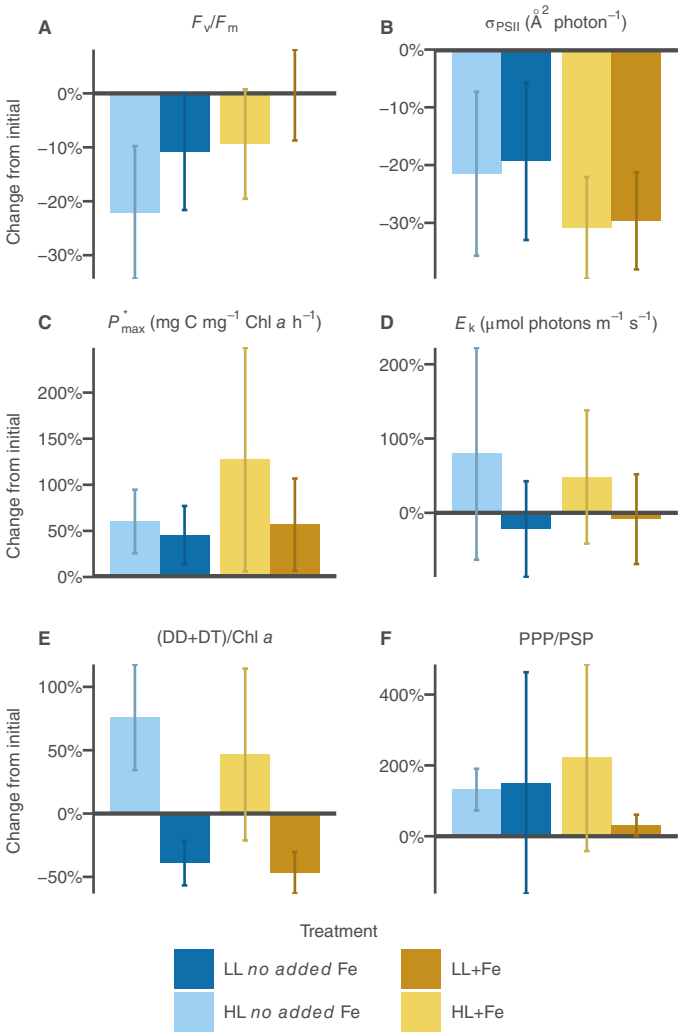

Fig. 4. Photosynthetic response to light treatment (HL, LL) and dissolved Fe (+Fe) additions shown in percent changes from initial averaged across experiments for (**a**) F_v/F_m: maximum photochemical efficiency of photosystem II (unitless), (**b**) σ_{PSII}: effective absorption cross section of photosystem II (Å^2 photon^{-1}), (**c**) P^*_{max}: maximum photosynthetic rate (mg C mg^{-1} Chl a h^{-1}), (**d**) E_k: photoacclimation parameter (µmol photons m^{-2} s^{-1}), (**e**) (DD + DT)/Chl a: ratio of diadinoxanthin and diatoxanthin to chlorophyll a (unitless), and (**f**) PPP/PSP: ratio of photoprotective pigments to photosynthetic pigment (unitless). Bar height represents mean and error bars show 1 standard deviation.

Carbon fixation characteristics

We did not *see* evidence of effects of light or Fe treatments or interactive effects on the carbon fixation parameters (P^*_{max}, α*, E_k, and ϕ_m; Fig. 4c,d; Table 2). On Day 0, P^*_{max} was high, ranging from 2.06 to 3.56 mg C mg^{-1} Chl a h^{-1} (mean: 2.85 ± 0.61 mg C mg^{-1} Chl a h^{-1}; Fig. 4c), but still increased in all treatments (mean: 4.75 ± 1.97 mg C mg^{-1} Chl a^{-1} h^{-1}) by Day 6 (*see* Supporting Information Table S2 for values).

Values for α* on Day 0 ranged from 0.019 to 0.059 mg C mg^{-1} Chl a h^{-1} (µmol photons m^{-2} s^{-1})$^{-1}$ (mean: 0.036 ±0.018 mg C mg^{-1} Chl a h^{-1} [µmol photons m^{-2} s^{-1}]$^{-1}$) and were unchanged in the LL + Fe treatment (0.038 ± 0.011 mg C mg^{-1} Chl a h^{-1} [µmol photons m^{-2} s^{-1}]$^{-1}$). However, α* increased in all other treatments, especially in the LL *no added* Fe treatment (0.080 ± 0.027 mg C mg^{-1} Chl a h^{-1} [µmol photons m^{-2} s^{-1}]$^{-1}$; Supporting Information Table S2).

On Day 0, E_k varied widely, from 34.8 to 187.2 µmol photons m^{-2} s^{-1} (mean: 102 ± 59 µmol photons m^{-2} s^{-1}). In the HL treatments, E_k increased slightly to 116 ± 20 µmol photons m^{-2} s^{-1} by Day 6 and decreased in LL treatments to 60 ± 14 µmol photons m^{-2} s^{-1}. It is notable that E_k was two times higher in HL than in LL treatments, an expected physiological effect of the light treatment, but due to high variability the difference was not significant.

On Day 0, ϕ_m ranged from 0.033 to 0.189 mol C (mol quanta absorbed)$^{-1}$ (mean: 0.094 ± 0.060 mol C (mol quanta absorbed)$^{-1}$). By Day 6, ϕ_m had increased more in the LL treatments (0.172 ± 0.073 mol C (mol quanta absorbed)$^{-1}$) than in HL treatments (0.105 ± 0.049 mol C (mol quanta absorbed)$^{-1}$). Although the theoretical upper limit for carbon fixation is 0.125 mol C (mol quanta absorbed)$^{-1}$ (Falkowski and Raven 2007), previous lab work on *P. antarctica* measured ϕ_m values higher than 0.125 mol C (mol quanta absorbed)$^{-1}$, ranging from 0.02 ± 0.005 mol C (mol quanta absorbed)$^{-1}$ in *Fragilariopsis cylindrus* (a common Antarctic diatom) to 0.10 ± 0.15 and 0.14 ± 0.017 mol C (mol quanta absorbed)$^{-1}$ for two strains of *P. antarctica* in simulated medium mixed layer depths (Mills et al. 2010). The average ϕ_m across all samples was 0.12 ± 0.07 mol C (mol quanta absorbed)$^{-1}$, within range of the *P. antarctica* values measured by Mills et al. (2010). Our samples were largely *P. antarctica* dominated, thus we expect our ϕ_m to be closer to the *P. antarctica* than the diatom values measured by Mills et al. (2010), while the large standard deviation reflects the presence of some diatom-dominated samples.

Light and Fe effects on accessory pigments

Across all experiments, photoprotective pigments increased in HL treatments. Specifically, (DD + DT)/Chl a, a measure of the xanthophyll cycle pigments used to reduce photodamage by dissipating excess energy, increased relative to Day 0 (0.121 ± 0.050; Fig. 4e; Supporting Information Table S2) in HL treatments (0.188 ± 0.074) and decreased in LL treatments (0.065 ± 0.020). Overall, (DD + DT)/Chl a was much higher in HL than in LL treatments ($p < 0.001$; Table 2). In addition, (DD + DT)/Chl a was higher without Fe addition (0.137 ± 0.087) than in the +Fe treatments (0.116 ± 0.081; $p < 0.001$; Table 2). (DD + DT)/Chl a also showed an interactive effect between light and Fe addition. (DD + DT)/Chl a was higher ($p = 0.012$; Table 2) in the HL *no added* Fe treatment (0.204 ± 0.071) than in either the HL treatment (0.188 ± 0.074) or the treatments without added Fe (0.137 ± 0.087).

The ratio of PPP to PSP increased in all treatments relative to Day 0 (0.090 ± 0.028; Fig. 4f; Supporting Information Table S2) and was also higher in HL (0.222 ± 0.079) than in LL (0.141 ± 0.099) treatments ($p < 0.001$; Table 2). Unlike (DD + DT)/Chl *a*, PPP/PSP did not respond to Fe addition, likely because *β*-carotene (a significant component of PPP but not represented in DD + DT) showed no Fe treatment effect. Similarly, PPP/PSP did not show an interactive effect between light and Fe.

Light and Fe effects on species composition

There were no treatment effects on species composition (Table 2), so we grouped treatments within an experiment to compare species composition between Days 0 and 6 in each experiment. In Experiments 1, 2, and 3 the relative abundance by biovolume of *P. antarctica* increased from Day 0 to Day 6, and in most of the experiments *P. antarctica* dominated throughout the experiment (Fig. 5a; Supporting Information Fig. S1; Table S2). Because the species composition changes were relatively small, the observed changes in experimental parameters are more attributable to growth than to taxa differences.

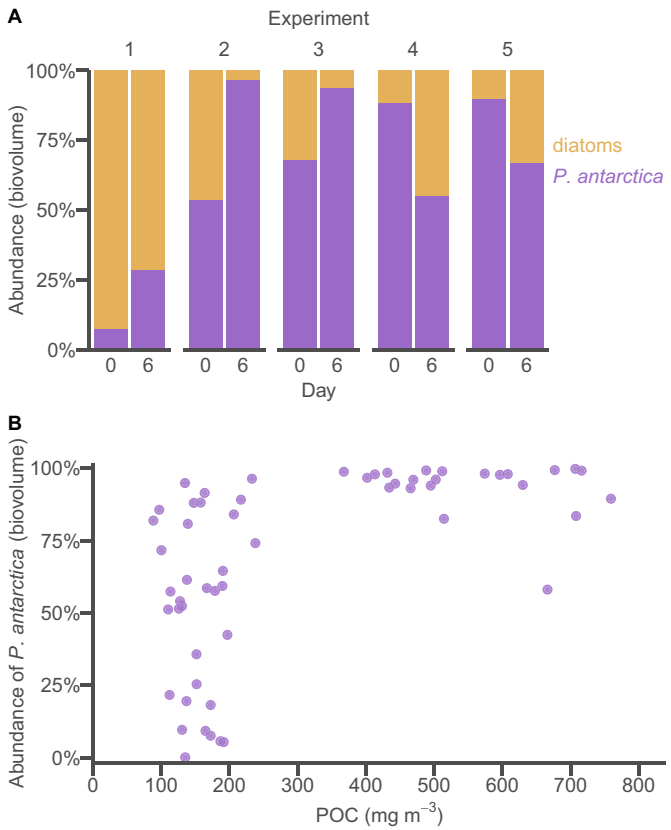

Fig. 5. (**a**) Species composition by biovolume on Days 0 and 6 in each experiment. Diatoms shown in yellow and *Phaeocystis antarctica* shown in purple. (**b**) Abundance of *P. antarctica* in each sample as a function of POC concentration in the same sample.

Within treatments, high POC concentrations (> 350 mg m^{-3}) were consistently associated with *P. antarctica* dominance (Fig. 5b). In contrast, at POC concentrations below 250 mg m^{-3}, there was no pattern in species composition of the samples (Fig. 5b).

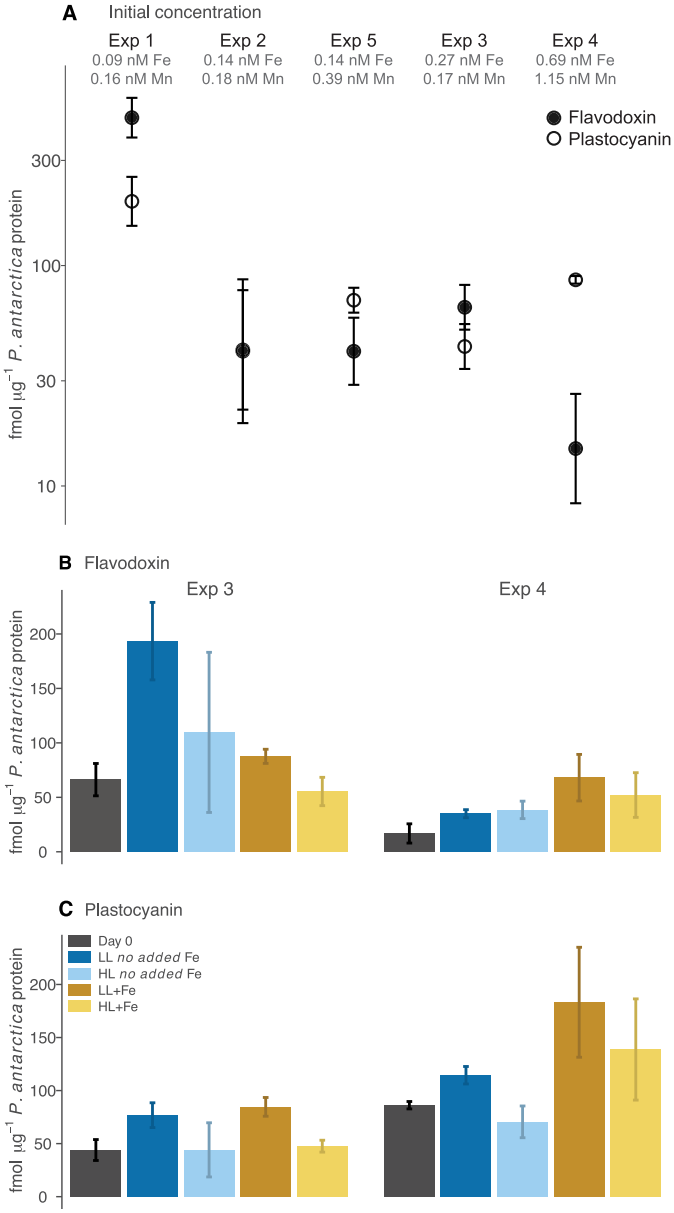

Fig. 6. (**a**) Flavodoxin (filled points) and plastocyanin (open points) concentrations (fmol μg^{-1} *Phaeocystis antarctica* protein) on Day 0. Experiments are arranged on the *x*-axis from lowest to highest in situ dissolved iron (Fe) concentrations, with in situ dissolved Fe (top row) and dissolved manganese (Mn; bottom row) concentrations in each experiment. The *y*-axis is log-transformed for clarity. (**b**) Flavodoxin and (**c**) plastocyanin concentrations (fmol μg^{-1} *P. antarctica* protein) on Day 0 and Day 4 following light treatment (HL, LL) and dissolved Fe (+Fe) additions. Points (**a**) and column heights (**b**, **c**) represent biological replicate means and error bars represent 1 standard deviation. Experiment 3 was conducted on-shelf; Experiment 4 was conducted off-shelf.

Protein expression patterns

To understand micronutrient stress through protein expression patterns, we quantified three *P. antarctica*-specific peptides that provide insight into metal stress, and one diatom-specific peptide that provides insight into vitamin B_{12} nutritional status (described in Supporting Information Section S3) for all experiments on Day 0 and on Day 4 for Experiment 3 (conducted on-shelf) and Experiment 4 (conducted off-shelf) (Supporting Information Tables S1 and S5). *P. antarctica* rubisco small subunit peptide (RbcS) concentrations were positively correlated with *P. antarctica* protein concentrations and were higher, relative to total *P. antarctica* protein, in the LL treatments ($p = 0.08$) (Supporting Information Fig. 5). On Day 0, *P. antarctica* flavodoxin and plastocyanin were most abundant under the lowest dissolved Fe concentrations and negatively correlated with dissolved Fe (Fig. 6a). After 4 d of incubation, *P. antarctica* flavodoxin expression, normalized to total *P. antarctica* protein abundance, was lower in the +Fe treatments than in the *no added* Fe treatments only in Experiment 3 ($p = 0.0033$). We did not observe any effects of light on flavodoxin expression in either experiment. In Experiment 3, plastocyanin abundance was greater in LL than in HL treatments ($p = 0.0175$), but was not influenced by Fe addition. In contrast, normalized plastocyanin expression in Experiment 4 was higher in the +Fe treatments than in the *no added* Fe treatments ($p = 0.0087$), but was not influenced by light level (Fig. 6c).

Diatom methionine synthase (MetE) peptide expression, normalized to total diatom protein abundance, on Day 0 was highest in Experiments 3, 4, and 5, and increased greatly on Day 4 in Experiment 3 (on-shelf) but not in Experiment 4 (off-shelf; Supporting Information Fig. S6). In addition, +Fe incubations in Experiment 3 had more MetE than incubations without added Fe ($p = 0.0011$).

Discussion

In the Southern Ocean, light and Fe availability control phytoplankton production. The cellular needs for light and Fe are intertwined because cells can photoacclimate by altering Fe-containing proteins (MacIntyre et al. 2000). In our bioassay experiments, we observed significant impacts of light treatment on phytoplankton biomass, growth, variable fluorescence, and photoprotective pigments, but not on carbon fixation parameters or species composition. We observed no significant impact of Fe addition on nutrient drawdown and biomass production and few interactive effects between light and Fe treatments, except for on maximum efficiency of PSII, photoprotective pigments, and protein expression. This indicates that phytoplankton were Fe-stressed (i.e., utilized various proteins and physiological mechanisms to maximize growth under low Fe availability; Behrenfeld and Milligan 2013), but despite relatively low Fe availability, were not Fe-limited (i.e., unable to maintain maximum growth rate or yield due to low Fe availability). We employed bioassay experiments and measured both photosynthetic parameters and micronutrient stress-induced protein expression to gain a new depth of insight into phytoplankton acclimation to LL and Fe availability. We demonstrate that, although light increased phytoplankton growth, springtime phytoplankton had very high maximum photosynthesis. Simultaneously, despite low Fe availability and indications of Fe-stress, phytoplankton were remarkably not Fe-limited.

Light and Fe effects on phytoplankton growth, biomass, and photosynthesis

The response of phytoplankton (in nutrients, biomass parameters, F_v/F_m, and pigments) to the HL treatments indicates that cells were acclimated to LL in the spring. In addition, these LL levels were limiting to phytoplankton growth, as we observed higher POC-based growth rate in HL than in LL treatments. The ratio of POC to PON decreased in HL and at higher growth rates, indicating that PON increased more than POC due to cells taking up NO_3^- faster than they were assimilating carbon. Correspondingly, NO_3^- was drawn down more in HL than in LL treatments. N in growth-related macromolecules (such as proteins, amino acids, and ribosomal RNA) likely increased, more than compensating for a reduction in high N-containing pigments, such as Chl *a*, in HL (Geider and LaRoche 2002; Arrigo 2005).

Chl *a* increased more in LL treatments than in HL treatments, indicating up-regulation of photosynthetic pigments to capture more light. Both (DD + DT)/Chl *a* and PPP/PSP were higher in HL than in LL treatments, showing that phytoplankton up-regulated these photoprotective pigments to reduce photodamage in HL. Similarly, POC/Chl *a* was higher in HL than in LL, consistent with a decrease in cellular Chl *a* concentration as a photoacclimation response to HL.

Although our results indicate that cells were acclimated to LL at the time of collection (high F_v/F_m and σ_{PSII}, low PPP/PSP), they were also photosynthetically optimized to light levels much greater than they were experiencing in situ (high P^*_{max} and E_k; Supporting Information Table S2), as was also observed in the Chukchi Sea (Lewis et al. 2018). Photosynthetic parameters (P^*_{max}, $\alpha^\star$, E_k, ϕ_m) did not change among treatments, likely because they were already quite high. These results, along with a high initial (DD + DT)/Chl *a* pool, indicate acclimation to a highly dynamic light regime, requiring efficient light harvesting and a high abundance of Calvin cycle enzymes to photosynthesize during alternating periods of low irradiance and saturating irradiance (Boelen et al. 2011). In situ measurements also showed increasing *P. antarctica* RbcS expression with increasing mixed layer depth (Supporting Information Fig. S7). This further suggests that cells adjusted Calvin cycle enzyme expression to maximize carbon fixation under the different light regimes in their environment. Thus, while phytoplankton appeared to be LL

acclimated, they were photosynthetically optimized to take advantage of any increase in light.

Low Day 0 Fe concentrations did not appear to influence the response of phytoplankton biomass and growth to light availability. However, Fe additions affected photophysiology: F_v/F_m was higher in +Fe treatments, while σ_{PSII} was lower in +Fe treatments, indicating that phytoplankton acclimated their photosystems based on Fe availability. This is in good agreement with summer photophysiological data showing low F_v/F_m and high σ_{PSII} in the continental slope region of the western Antarctic Peninsula (low Fe) and high F_v/F_m and low σ_{PSII} near the coast (high Fe) (Sherman et al. 2020). Note that because F_v/F_m decreased in all treatments relative to Day 0, this line of evidence alone may indicate that phytoplankton were not Fe-stressed in situ, but rather that Fe-stress was later induced during the incubations. However, combined with higher in situ measurements of flavodoxin and plastocyanin expression off-shelf (lower dissolved Fe) than on-shelf (higher dissolved Fe), as well as a decrease in *P. antarctica* flavodoxin expression, σ_{PSII}, and (DD + DT)/Chl *a* over the experiments, the observed higher F_v/F_m in +Fe treatments suggests that phytoplankton were likely Fe-stressed in situ.

In addition, (DD + DT)/Chl *a* was lower in the LL and +Fe treatments. More coupled (active) reaction centers in LL and with added Fe (evidenced in higher F_v/F_m) reflect increased potential for carbon fixation, thus reducing the backlog of electrons needing to be dissipated via photoprotective pathways, such as xanthophyll cycling (leading to lower (DD + DT)/Chl *a*) (Demmig-Adams 1990). This suggests that prior to incubations, *P. antarctica* cells were Fe-stressed and used Fe-conserving strategies such as replacing Fe-containing ferredoxin with flavodoxin and Fe-containing cytochrome c_6 with plastocyanin to support growth (LaRoche et al. 1996; Peers and Price 2006). Although these expression patterns are indicative of Fe-stress in *P. antarctica*, some polar diatoms lack evidence of a ferredoxin gene (Pankowski and McMinn 2009) and may constitutively express flavodoxin under a wide range of Fe conditions. These proteins can further reduce the backlog of electrons by facilitating electron movement and photosynthesis under low Fe availability. Iron addition led to decreased flavodoxin expression, fewer uncoupled reaction centers (increased F_v/F_m) and smaller antennae (lower σ_{PSII}), which is a typical response of cells that are Fe-limited (Greene et al. 1991; Jabre and Bertrand 2020). Although variability in F_v/F_m and σ_{PSII} is often dominated by changes in species composition in much of the world's oceans, in high nutrient low chlorophyll regions such as the Southern Ocean, the dominant changes in F_v/F_m and σ_{PSII} are in response to changes in ambient Fe concentration (Suggett et al. 2009).

Our findings are consistent with hypothesized patchy Fe-limited phytoplankton production in the summertime along the western Antarctic Peninsula (Garibotti et al. 2003). Lending support to this hypothesis, Annett et al. (2017) measured low and spatially heterogeneous coastal summer dissolved Fe concentrations and showed that coastal summer dissolved Fe inputs are attenuated rapidly offshore. Our results compliment this understanding by demonstrating spring Fe-stress prior to possible summer Fe limitation, with high dissolved Fe variability. In addition, flavodoxin and plastocyanin protein expression was much higher in phytoplankton originating off-shelf (low dissolved Fe) than on-shelf (high dissolved Fe) (Fig. 6a), indicating springtime Fe-stress in areas along the western Antarctic Peninsula that are less influenced by shelf sources of Fe. The decrease in flavodoxin expression in off-shelf (low dissolved Fe) but not on-shelf (high dissolved Fe) in +Fe treatments relative to *no added* Fe treatments (Fig. 6b) further indicates that on-shelf phytoplankton were experiencing Fe-replete conditions, while off-shelf phytoplankton were experiencing Fe-stress.

In addition to *P. antarctica*-specific proteins, we measured the expression of diatom-specific vitamin B_{12}-independent methionine synthase (MetE). MetE is used in some diatoms to synthesize the essential amino acid methionine under low vitamin B_{12} availability, making it a reliable marker for low vitamin B_{12} availability (Bertrand et al. 2012; Ellis et al. 2017). In situ expression of MetE in our study ranged from values previously observed in the Ross Sea ($\sim$ 0.1–0.5 fmol μg^{-1} bulk protein under diatom dominated conditions; Bertrand et al. 2013) to much higher concentrations ($\sim$ 0.5–8 fmol μg^{-1} diatom protein), which is consistent with stress due to lack of vitamin B_{12} (Bertrand et al. 2012). This suggests that the diatoms present at the initiation of Experiments 3, 4, and 5 were experiencing stress due to low vitamin B_{12}, perhaps contributing to the continued dominance of *P. antarctica*, which is likely less impacted by low B_{12} availability (Bertrand et al. 2007; Bertrand et al. 2013). Fe addition in off-shelf (low dissolved Fe), but not on-shelf (high dissolved Fe) experiments (Supporting Information Fig. S6), resulted in a large increase in diatom MetE. This suggests that with added Fe, vitamin B_{12} stress increased due to increased vitamin B_{12} demand by phytoplankton. These proteomic measurements are consistent with the increase in MetE transcript abundance resulting from Fe addition in natural phytoplankton assemblages in the Ross Sea (Bertrand et al. 2015) and the North Pacific (Marchetti et al. 2012; Cohen et al. 2017). The ability to utilize MetE can give some diatoms an advantage during natural iron fertilization events and highlights the role that vitamin B_{12} and Fe dynamics play in interactively controlling stoichiometry (Koch and Trimborn 2019) and species composition in the springtime western Antarctic Peninsula. Future experiments assessing vitamin B_{12} concentrations, bacterial community composition and responses to changing Fe availability would help elucidate the relationships between light, trace metals, vitamin B_{12}, and phytoplankton growth along the western Antarctic Peninsula during springtime.

Given that Fe is usually considered the limiting nutrient in the Southern Ocean, it is noteworthy that Mn was drawn down to similar or even lower concentrations. The depletion

of dissolved Mn to values as low as 0.02 nmol L^{-1} and up to 84% of the starting concentration indicates that Mn was a crucial nutrient for the community. Wu et al. (2019) show increased flavodoxin expression under low Fe conditions only when Mn concentrations were non-limiting. Here, flavodoxin expression was high under low Fe even when dissolved Mn was relatively low (Fig. 6a; Supporting Information Fig. S4), suggesting that *P. antarctica* may not have been Mn-limited under the observed dissolved Mn conditions, or that there are important strain-specific variations in *P. antarctica* protein responses to micronutrient stress, as identified by Bender et al. (2018) when considering *P. antarctica* responses to Fe alone. The greater relative dissolved Mn drawdown in most experiments under HL, notably without Fe addition, as well as the relationship between dissolved Mn and F_v/F_m, indicates that there is an interaction between Mn, light, and Fe. However, no consistent effect of light or Fe was observed on dissolved Mn drawdown, suggesting the effects on Mn, as for Fe, varies spatially and likely temporally as well. This finding is consistent with other studies on Mn (co-)limitation that also found inconsistent effects of Mn additions (e.g., Wu et al. 2019) or no effect at all (Martin et al. 1990).

Interaction among light, Fe, and Mn

Two major known sinks for Mn in cells include the PSII water-splitting center and Mn superoxide dismutase (MnSOD) (Raven 1990). Increased Mn drawdown under HL (Supplemental Table 3) could indicate that more PSII Mn-containing reaction centers are formed when more light is available to fuel carbon fixation. However, Wu et al. (2019) observed that PSII protein expression in *P. antarctica* is independent of Mn availability, suggesting that Fe, not Mn, drives PSII abundance patterns. Moreover, given that there is no detectable effect of Fe additions on Mn drawdown and Mn drawdown is negatively related to F_v/F_m (highest Mn drawdown at the lowest F_v/F_m; Supporting Information Fig. S4a), these observations may instead be driven by another biochemical role for Mn, such as SOD. In SOD, Mn aids in quenching harmful superoxide anion radicals (O_2^-), which are thought to increase under Fe limitation (Wolfe-Simon et al. 2005; Middag et al. 2013; Kaushik et al. 2015) and when F_v/F_m is low (Peers and Price 2004). The increased Mn drawdown under elevated light observed in this study suggests that higher light levels might increase demand for MnSOD. Under both low Fe availability and HL stress, the formation of reactive oxygen species becomes more prevalent: electrons that are formed as part of the photosynthetic pathway are less efficiently transferred with a higher chance of forming radicals (Peers and Price 2004). Albeit a plausible explanation for the observed Mn trends in these experiments, further targeted experiments are needed to unravel the elusive role of Mn in the Southern Ocean phytoplankton community.

Dissolved Mn drawdown was related to indicators of growth and was greatest when relative abundance of *P. antarctica* was highest, likely due in part to the greater abundance of *P. antarctica* at higher POC concentrations and growth rates. Colonial *P. antarctica* sequestering Mn into its mucilaginous matrix may contribute to elevated dissolved Mn drawdown with high *P. antarctica* abundance (Lubbers et al. 1990; Schoemann et al. 2001). However, *P. antarctica* abundance did not respond to light or Fe treatments, while Mn drawdown was slightly elevated in HL, indicating that other factors, including Mn photoreduction, may influence the interaction among light, Mn, and Fe availability.

Species composition

Although we did not observe an impact of either light or Fe treatment on species composition, given our measured growth rates of 0.15–0.20 d^{-1}, a species composition shift would need to be quite strong to be observed. However, *P. antarctica* was consistently dominant in samples with high biomass and increased or remained dominant in most experiments, indicating that *P. antarctica* may be better acclimated for early season growth when light can change dramatically in short periods of time given deep mixed layers and melting sea ice (Kropuenske et al. 2009; Rozema et al. 2017). Related work also demonstrated that *P. antarctica* growth (but not diatom growth) was stimulated by short periods of HL exposure (simulating transient mixing from the bottom to the top of the mixed layer) (Joy-Warren et al. 2019). Although spatial variability of dissolved Fe is high in the coastal western Antarctic Peninsula in both the spring (this study) and summer (Annett et al. 2017), our results showing *P. antarctica* dominance are consistent with the ability of *P. antarctica* to grow under low and varying irradiance and varying Fe concentrations (Trimborn et al. 2019).

Although this and accompanying studies (Arrigo et al. 2017; Selz et al. 2018; Joy-Warren et al. 2019) demonstrate that *P. antarctica* dominates the phytoplankton community along the western Antarctic Peninsula during spring, previous work in the PAL-LTER region has shown that diatoms dominate in the summer (Garibotti et al. 2003; Trimborn et al. 2015). This transition is potentially driven by a shift from *P. antarctica*-favored lower and more variable light due to deep mixed layers and lower incident light to diatom-favored higher and more consistent light as incident light increases into summer and the mixed layer shoals with melting sea ice (Kropuenske et al. 2009; Rozema et al. 2017). However, there are other factors at play in determining taxa dominance, possibly including vitamin B_{12}, as low vitamin B_{12} restricts diatom growth but is thought to have little impact on *P. antarctica* (Bertrand et al. 2007).

Future implications

The atmospheric and oceanic conditions in the western Antarctic Peninsula are changing rapidly and dramatically

(Schofield et al. 2010), and both light and Fe availability are susceptible to these changes. Sea ice directly impacts light penetration and indirectly impacts stratification, thereby determining the amount of light to which phytoplankton are exposed. A trend of increasing sea ice concentration (Schofield et al. 2018) could lead to enhanced stratification and thus elevated light availability throughout a shallower mixed layer. Moreover, Annett et al. (2017) predicted that meteoric and subglacial Fe supply may increase with a warming climate. However, it is unclear whether this additional Fe supply to the surface ocean will become more diluted because of mixed layer deepening (Venables et al. 2013) or more concentrated because of mixed layer shoaling (Schofield et al. 2018).

In the near future, phytoplankton may have access to both increased light and Fe in the waters along the western Antarctic Peninsula, which might favor *P. antarctica* early in the growing season, with a seasonal transition to diatoms later in the season as light availability increases and stable. Such predictions remain speculative, but most likely, changing conditions in the western Antarctic Peninsula will alter the timing and possibly degree of *P. antarctica* and diatom dominance of the phytoplankton community. Although there are likely complex interactions between light and Fe on phytoplankton growth and species composition, in addition to other possibly limiting nutrients including Mn and vitamin B_{12}, our results demonstrate for the first time that early in the growing season, light exerts the most control on phytoplankton populations along the western Antarctic Peninsula. Our results highlight that further targeted experiments are needed to resolve the role of Mn and vitamin B_{12} in the Southern Ocean phytoplankton community.

Conclusions

In our study in the spring along the western Antarctic Peninsula, phytoplankton growth was light-limited and the community was dominated by *P. antarctica*. Phytoplankton were LL acclimated at the time of collection but were photosynthetically optimized for light much greater than they were experiencing in situ, and as a result, photosynthetic parameters (P^*_{max}, α^*, E_k, ϕ_m) did not respond to the HL treatment. Overall, there was a limited response to Fe addition, indicating that phytoplankton were not Fe-limited, but somewhat Fe-stressed (evident in increased F_v/F_m, decreased σ_{PSII}, and decreased (DD + DT)/Chl *a* with Fe addition relative to *no added* Fe). Our observations of *P. antarctica* dominance differ from what has been shown along the western Antarctic Peninsula in the summer when light is no longer limiting and diatoms dominate. This new understanding of light, Fe, Mn, vitamin B_{12}, and species composition in the spring adds an important component to our understanding of micronutrient-induced stress in phytoplankton communities and seasonal phytoplankton taxa succession in the western Antarctic Peninsula ecosystem.

References

Alderkamp, A.-C., and others. 2019. Effects of iron and light availability on phytoplankton photosynthetic properties in the Ross Sea. Mar. Ecol. Prog. Ser. **621**: 33–50. doi:10.3354/meps13000

Annett, A. L., D. S. Carson, X. Crosta, A. Clarke, and R. S. Ganeshram. 2010. Seasonal progression of diatom assemblages in surface waters of Ryder Bay, Antarctica. Polar Biol. **33**: 13–29. doi:10.1007/s00300-009-0681-7

Annett, A. L., M. Skiba, S. F. Henley, H. J. Venables, M. P. Meredith, P. J. Statham, and R. S. Ganeshram. 2015. Comparative roles of upwelling and glacial iron sources in Ryder Bay, coastal western Antarctic Peninsula. Mar. Chem. **176**: 21–33. doi:10.1016/j.marchem.2015.06.017

Annett, A. L., J. N. Fitzsimmons, M. J. M. Séguret, M. Lagerström, M. P. Meredith, O. M. Schofield, and R. M. Sherrell. 2017. Controls on dissolved and particulate iron distributions in surface waters of the Western Antarctic Peninsula shelf. Mar. Chem. **196**: 81–97. doi:10.1016/j.marchem.2017.06.004

Arrigo, K. R. 2005. Marine microorganisms and global nutrient cycles. Nature **437**: 349–356. doi:10.1038/nature0415

Arrigo, K. R., D. H. Robinson, D. L. Worthen, R. B. Dunbar, G. R. DiTullio, M. VanWoert, and M. P. Lizotte. 1999. Phytoplankton community structure and the drawdown of nutrients and CO_2 in the Southern Ocean. Science **283**: 365–367. doi:10.1126/science.283.5400.365

Arrigo, K. R., M. M. Mills, L. R. Kropuenske, G. L. Van Dijken, A.-C. Alderkamp, and D. H. Robinson. 2010. Photophysiology in two major Southern Ocean phytoplankton taxa: Photosynthesis and growth of *Phaeocystis antarctica* and *Fragilariopsis cylindrus* under different irradiance levels. Integr. Comp. Biol. **50**: 950–966. doi:10.1093/icb/icq021

Arrigo, K. R., and others. 2017. Early spring phytoplankton dynamics in the Western Antarctic Peninsula. J. Geophys. Res. Ocean. **122**: 1–20. doi:10.1002/2017JC013281

Behrenfeld, M. J., and A. J. Milligan. 2013. Photophysiological expressions of iron stress in phytoplankton. Ann. Rev. Mar. Sci. **5**: 217–246. doi:10.1146/annurev-marine-121211-172356

Bender, S. J., and others. 2018. Colony formation in *Phaeocystis antarctica* connecting molecular mechanisms with iron biogeochemistry. Biogeosciences **15**: 4923–4942. doi:10.5194/bg-15-4923-2018

Bertrand, E. M., M. A. Saito, J. M. Rose, C. R. Riesselman, M. C. Lohan, A. E. Noble, P. A. Lee, and G. R. DiTullio. 2007. Vitamin B12 and iron colimitation of phytoplankton growth in the Ross Sea. Limnol. Oceanogr. **52**: 1079–1093. doi:10.4319/lo.2007.52.3.1079

Bertrand, E. M., A. E. Allen, C. L. Dupont, T. M. Norden-Krichmar, J. Bai, R. E. Valas, and M. A. Saito. 2012. Influence of cobalamin scarcity on diatom molecular physiology and identification of a cobalamin acquisition protein. Proc. Natl. Acad. Sci. **109**: E1762–E1771. doi:10.1073/pnas.1201731109

Bertrand, E. M., D. M. Moran, M. R. McIlvin, J. M. Hoffman, A. E. Allen, and M. A. Saito. 2013. Methionine synthase interreplacement in diatom cultures and communities: Implications for the persistence of B_{12} use by eukaryotic phytoplankton. Limnol. Oceanogr. **58**: 1431–1450. doi:10.4319/lo.2013.58.4.1431

Bertrand, E. M., and others. 2015. Phytoplankton–bacterial interactions mediate micronutrient colimitation at the coastal Antarctic Sea ice edge. Proc. Natl. Acad. Sci. **112**: 9938–9943. doi:10.1073/pnas.1501615112

Boelen, P., W. H. van de Poll, H. J. van der Strate, I. A. Neven, J. Beardall, and A. G. J. Buma. 2011. Neither elevated nor reduced CO_2 affects the photophysiological performance of the marine Anarctic diatom *Chaetoceros brevis*. J. Exp. Mar. Biol. Ecol. **406**: 38–45.

Boyd, P. W., K. R. Arrigo, R. F. Strzepek, and G. L. Van Dijken. 2012. Mapping phytoplankton iron utilization: Insights into Southern Ocean supply mechanisms. J. Geophys. Res. Ocean. **117**: 1–18. doi:10.1029/2011JC007726

Cohen, N. R., K. A. Ellis, W. G. Burns, R. H. Lampe, N. Shuback, Z. Johnson, S. Sañudo-Wilhelmy, and A. Marchetti. 2017. Iron and vitamin interactions in marine diatom isolates and natural assemblages of the Northeast Pacific Ocean. Limnol. Oceanogr. **62**: 2076–2096. doi:10.1002/lno.10552

Demmig-Adams, B. 1990. Carotenoids and photoprotection in plants: A role for the xanthophyll zeaxanthin. Biochim. Biophys. Acta **1020**: 1–24. doi:10.1016/0005-2728(90)90088-L

Ducklow, H. W., and others. 2007. Marine pelagic ecosystems: The west Antarctic Peninsula. Philos. Trans. R. Soc. Lond. B Biol. Sci. **362**: 67–94. doi:10.1098/rstb.2006.1955

Eberhard, S., G. Finazzi, and F.-A. Wollman. 2008. The dynamics of photosynthesis. Annu. Rev. Genet. **42**: 463–515. doi:10.1146/annurev.genet.42.110807.091452

Ellis, K. A., N. R. Cohen, C. Moreno, and A. Marchetti. 2017. Cobalamin-independent methionine synthase distribution and influence on vitamin B_{12} growth requirements in marine diatoms. Protist **168**: 32–47. doi:10.1016/j.protis.2016.10.007

Falkowski, P. G., and J. A. Raven. 2007. Aquatic photosynthesis, 2nd ed. Princeton Univ. Press. doi:10.1038/nrmicro1751

Fisher, A. C., J. J. Kroon, T. G. Verburg, T. Teunissen, and H. T. Wolterbeek. 2007. On the relevance of iron adsorption to container materials in small-volume experiments on iron marine chemistry: ^{55}Fe-aided assessment of capacity, affinity and kinetics. Mar. Chem. **107**: 533–546. doi:10.1016/j.marchem.2007.08.004

Garibotti, I. A., M. Vernet, M. E. Ferrario, R. C. Smith, R. M. Ross, and L. B. Quetin. 2003. Phytoplankton spatial distribution patterns along the western Antarctic Peninsula (Southern Ocean). Mar. Ecol. Prog. Ser. **261**: 21–39. doi:10.3354/meps261021

Geider, R. J., and J. LaRoche. 2002. Redfield revisited: Variability of C:N:P in marine microalgae and its biochemical basis. Eur. J. Phycol. **37**: 1–17. doi:10.1017/S0967026201003456

Gerringa, L. J. A., P. Laan, G. L. van Dijken, H. van Haren, H. J. W. de Baar, K. R. Arrigo, and A.-C. Alderkamp. 2015. Sources of iron in the Ross Sea Polynya in early summer. Mar. Chem. **177**: 447–459. doi:10.1016/j.marchem.2015.06.002

Gerringa, L. J. A., P. Laan, K. R. Arrigo, G. L. van Dijken, and A.-C. Alderkamp. 2019. The organic complexation of iron in the Ross Sea. Mar. Chem. **215**: 103672. doi:10.1016/j.marchem.2019.103672

Gerringa, L. J. A., A.-C. Alderkamp, G. L. Van Dijken, P. Laan, R. Middag, and K. R. Arrigo. 2020. Dissolved trace metals in the Ross Sea. Front. Mar. Sci. **7**: 874. doi:10.3389/fmars.2020.577098

Gorbunov, M. Y., Z. S. Kolber, and P. G. Falkowski. 1999. Measuring photosynthetic parameters in individual algal cells by fast repetition rate fluorometry. Photosynth. Res. **62**: 141–153. doi:10.1023/A:1006360005033

Greene, R. M., R. J. Geider, and P. G. Falkowski. 1991. Effect of iron limitation on photosynthesis in a marine diatom. Limnol. Oceanogr. **36**: 1772–1782. doi:10.4319/lo.1991.36.8.1772

Higgins, H. W., S. W. Wright, and L. Schlüter. 2011. Quantitative interpretation of chemotaxonomic pigment data, p. 257–313. *In* S. Roy, C. A. Llewellyn, E. S. Egeland, and G. Johnsen [eds.], Phytoplankton pigments: Characterization, chemotaxonomy and applications in oceanography. Cambridge Univ. Press. https://books.google.com/books?hl=en&lr=&id=K_2AJHmdvxgC&oi=fnd&pg=PR9&dq=Phytoplankton+pigments:+Characterization,+chemotaxonomy+and+applications+in+oceanography&ots=YmXsosv4E0&sig=KbuhXl3PrwMZPZpL_yzTaFK7F6s#v=onepage&q=Phytoplankton%20pigments%3A%20Characterization%2C%20chemotaxonomy%20and%20applications%20in%20oceanography&f=false

Jabre, L., and E. M. Bertrand. 2020. Interactive effects of iron and temperature on the growth of *Fragilariopsis cylindrus*. Limnol. Oceanogr. Lett. **5**: 363–370. doi:10.5061/dryad.np5hqbzq3

Joy-Warren, H. L., and others. 2019. Light is the primary driver of early season phytoplankton production along the western Antarctic Peninsula. J. Geophys. Res. Ocean **1–25**: 7375–7399. doi:10.1029/2019JC015295

Kaushik, M. S., M. Srivastava, E. Verma, and A. K. Mishra. 2015. Role of manganese in protection against oxidative stress under iron starvation in cyanobacterium *Anabaena* 7120. J. Basic Microbiol. **7120**: 729–740. doi:10.1002/jobm.201400742

Koch, F., and S. Trimborn. 2019. Limitation by Fe, Zn, Co, and B_{12} results in similar physiological responses in two Antarctic phytoplankton species. Front. Mar. Sci. **6**: 1–17.

Kropuenske, L. R., M. M. Mills, G. L. van Dijken, S. Bailey, D. H. Robinson, N. A. Welschmeyer, and K. R. Arrigo. 2009. Photophysiology in two major Southern Ocean phytoplankton taxa: Photoprotection in *Phaeocystis antarctica* and *Fragilariopsis cylindrus*. Limnol. Oceanogr. **54**: 1176–1196. doi:10.4319/lo.2009.54.4.1176

Kwon, Y. S., H. S. La, J. Jung, S. H. Lee, T.-W. Kim, H.-W. Kang, and S. Lee. 2021. Exploring the roles of iron and irradiance in dynamics of diatoms and *Phaeocystis* in the Amundsen Sea continental shelf water. J. Geophys. Res. Ocean **126**: e2020JC016673. doi:10.1029/2020JC016673

LaRoche, J., P. W. Boyd, M. McKay, and R. Geider. 1996. Flavodoxin as an in situ marker for iron stress in phytoplankton. Nature **382**: 802–805. https://www.nature.com/articles/382802a0

Lewis, K. M., and others. 2018. Photoacclimation of Arctic Ocean phytoplankton to shifting light and nutrient limitation. Limnol. Oceanogr. **64**: 1–18. doi:10.1002/lno.11039

Lubbers, G. W., W. W. C. Gieskes, P. Castilho, W. Salomons, and J. Bril. 1990. Manganese accumulation in the high pH microenvironment of *Phaeocystis* sp. (Haptophyceae) colonies from the North Sea. Mar. Ecol. Prog. Ser. **59**: 285–293.

MacIntyre, H. L., T. M. Kana, and R. J. Geider. 2000. The effect of water motion on short-term rates of photosynthesis by marine phytoplankton. Trends Plant Sci. **5**: 12–17. doi:10.1016/S1360-1385(99)01504-6

Marchetti, A., D. M. Schruth, C. A. Durkin, M. S. Parker, R. B. Kodner, C. T. Berthiaume, R. Morales, A. E. Allen, and E. V. Armbrust. 2012. Comparative metatranscriptomics identifies molecular bases for the physiological responses of phytoplankton to varying iron availability. Proc. Natl. Acad. Sci. **109**: E317–E325. doi:10.1073/pnas.1118408109

Martin, J. H., S. E. Fitzwater, and R. M. Gordon. 1990. Iron deficiency limits phytoplankton growth in Antarctic waters. Global Biogeochem. Cycl. **4**: 5–12. doi:10.1029/GB004i001p00005

Middag, R., H. J. W. de Baar, M. B. Klunder, and P. Laan. 2013. Fluxes of dissolved aluminum and manganese to the Weddell Sea and indications for manganese co-limitation. Limnol. Oceanogr. **58**: 287–300. doi:10.4319/lo.2013.58.1.0287

Mills, M. M., and others. 2010. Photophysiology in two Southern Ocean phytoplankton taxa: Photosynthesis of *Phaeocystis Antarctica* (Prymnesiophyceae) and *Fragilariopsis cylindrus* (Bacillariophyceae) under simulated mixed-layer irradiance. J. Phycol. **46**: 1114–1127. doi:10.1111/j.1529-8817.2010.00923.x

Moline, M. A., H. Claustre, T. K. Frazer, O. M. Schofield, and M. Vernet. 2004. Alteration of the food web along the Antarctic Peninsula in response to a regional warming trend. Glob. Chang. Biol. **10**: 1973–1980. doi:10.1111/j.1365-2486.2004.00825.x

Murphy, E. J., E. E. Hofmann, J. L. Watkins, and others. 2013. Comparison of the structure and function of Southern Ocean regional ecosystems: The Antarctic Peninsula and South Georgia. J. Mar. Syst. **109–110**: 22–42. doi:10.1016/j.jmarsys.2012.03.011

Pankowski, A., and A. McMinn. 2009. Iron availability regulates growth, photosynthesis, and production of ferredoxin and flavodoxin in Antarctic Sea ice diatoms. Polar Biol. **4**: 273–288. doi:10.3354/ab00116

Peers, G., and N. M. Price. 2004. A role for manganese in superoxide dismutases and growth of iron-deficient diatoms. Limnol. Oceanogr. **49**: 1774–1783. doi:10.4319/lo.2004.49.5.1774

Peers, G., and N. M. Price. 2006. Copper-containing plastocyanin used for electron transport by an oceanic diatom. Nature **441**: 341–344. doi:10.1038/nature04630

Raven, J. A. 1990. Predictions of Mn and Fe use efficiencies of phototrophic growth as a function of light availability for growth and of C assimilation pathway. New Phytol. **116**: 1–18. doi:10.1111/j.1469-8137.1990.tb00505.x

Rozema, P. D., H. J. Venables, W. H. van de Poll, A. Clarke, M. P. Meredith, and A. G. J. Buma. 2017. Interannual variability in phytoplankton biomass and species composition in northern Marguerite Bay (West Antarctic Peninsula) is governed by both winter sea ice cover and summer stratification. Limnol. Oceanogr. **62**: 235–252. doi:10.1002/lno.10391

Saba, G. K., and others. 2014. Winter and spring controls on the summer food web of the coastal West Antarctic Peninsula. Nat. Commun. **5**: 1–8. doi:10.1038/ncomms5318

Schoemann, V., R. Wollast, L. Chou, and C. Lancelot. 2001. Effects of photosynthesis on the accumulation of Mn and Fe by *Phaeocystis* colonies. Limnol. Oceanogr. **46**: 1065–1076. doi:10.4319/lo.2001.46.5.1065

Schofield, O. M., H. W. Ducklow, D. G. Martinson, M. P. Meredith, M. A. Moline, and W. R. Fraser. 2010. How do polar marine ecosystems respond to rapid climate change? Science **328**: 1520–1523. doi:10.1126/science.1185779

Schofield, O. M., M. S. Brown, J. T. Kohut, S. Nardelli, G. K. Saba, N. Waite, and H. W. Ducklow. 2018. Changing upper ocean mixed layer depth and phytoplankton productivity along the West Antarctic Peninsula. Philos. Trans. R. Soc. A **376**: 1–12. doi:10.1098/rsta.2017.0173

Selz, V., and others. 2018. Distribution of *Phaeocystis Antarctica*-dominated sea ice algal communities and their potential to seed phytoplankton across the western Antarctic Peninsula in spring. Mar. Ecol. Prog. Ser. **586**: 91–112. doi:10.3354/meps12367

Sherman, J., M. Y. Gorbunov, O. Schofield, and P. G. Falkowski. 2020. Photosynthetic energy conversion

efficiency in the West Antarctic Peninsula. Limnol. Oceanogr. **65**: 2912–2925. doi:10.1002/lno.11562

Strzepek, R. F., M. T. Maldonado, K. A. Hunter, R. D. Frew, and P. W. Boyd. 2011. Adaptive strategies by Southern Ocean phytoplankton to lessen iron limitation: Uptake of organically complexed iron and reduced cellular iron requirements. Limnol. Oceanogr. **56**: 1983–2002. doi:10.4319/lo.2011.56.6.1983

Strzepek, R. F., K. A. Hunter, R. D. Frew, P. J. Harrison, and P. W. Boyd. 2012. Iron-light interactions differ in Southern Ocean phytoplankton. Limnol. Oceanogr. **57**: 1182–1200. doi:10.4319/lo.2012.57.4.1182

Strzepek, R. F., P. W. Boyd, and W. G. Sunda. 2019. Photosynthetic adaptation to low iron, light, and temperature in Southern Ocean phytoplankton. PNAS **116**: 4388–4393. doi:10.1073/pnas.1810886116

Suggett, D. J., C. M. Moore, A. E. Hickman, and R. J. Geider. 2009. Interpretation of fast repetition rate (FRR) fluorescence: Signatures of phytoplankton community structure versus physiological state. Mar. Ecol. Prog. Ser. **376**: 1–19. doi:10.3354/meps07830

Sunda, W. G., and S. A. Huntsman. 1997. Interrelated influence of iron, light and cell size on marine phytoplankton growth. Nature **390**: 389–392. doi:10.1038/37093

Trimborn, S., C. J. M. Hoppe, B. B. Taylor, A. Bracher, and C. S. Hassler. 2015. Physiological characteristics of open ocean and coastal phytoplankton communities of Western Antarctic Peninsula and Drake Passage waters. Deep. Res. Part I Oceanogr. Res. Pap. **98**: 115–124. doi:10.1016/j.dsr.2014.12.010

Trimborn, S., and others. 2017. Iron sources alter the response of Southern Ocean phytoplankton to ocean acidification. Mar. Ecol. Prog. Ser. **578**: 35–50. doi:10.3354/meps12250

Trimborn, S., S. Thoms, K. Bischof, and S. Beszteri. 2019. Susceptibility of two Southern Ocean phytoplankton key species to iron limitation and high light. Front. Mar. Sci. **6**: 1–17. doi:10.3389/fmars.2019.00167

Van Heukelem, L., and C. S. Thomas. 2001. Computer-assisted high-performance liquid chromatography method development with applications to the isolation and analysis of phytoplankton pigments. J. Chromatogr. A **910**: 31–49. doi:10.1016/S0378-4347(00)00603-4

Van Leeuwe, M. A., L. A. Villerius, J. Roggeveld, R. J. W. Visser, and J. Stefels. 2006. An optimized method for automated analysis of algal pigments by HPLC. Mar. Chem. **102**: 267–275. doi:10.1016/j.marchem.2006.05.003

Van Leeuwe, M. A., R. J. W. Visser, and J. Stefels. 2014. The pigment composition of *Phaeocystis antarctica* (Haptophyceae) under various conditions of light, temperature, salinity, and iron. J. Phycol. **50**: 1070–1080. doi:10.1111/jpy.12238

Van Leeuwe, M. A., A. L. Webb, H. J. Venables, R. J. W. Visser, M. P. Meredith, J. T. M. Elzenga, and J. Stefels. 2020. Annual patterns in phytoplankton phenology in Antarctic coastal waters explained by environmental drivers. Limnol. Oceanogr. **65**: 1651–1668. doi:10.1002/lno.11477

Venables, H. J., A. Clarke, and M. P. Meredith. 2013. Wintertime controls on summer stratification and productivity at the western Antarctic Peninsula. Limnol. Oceanogr. **58**: 1035–1047. doi:10.4319/lo.2013.58.3.1035

Wobbrock, J. O., L. Findlater, D. Gergle, and J. J. Higgins. 2011. The aligned rank transform for nonparametric factorial analyses using only ANOVA procedures. *In* Proceedings of the SIGCHI Conference on Human Factors in Computer Systems, pp. 143–146. Association for Computing Machinery. doi:10.1145/1978942.1978963

Wolfe-Simon, F., D. Grzebyk, O. M. Schofield, and P. G. Falkowski. 2005. The role and evolution of superoxide dismutases in algae. J. Phycol. **41**: 453–465. doi:10.1111/j.1529-8817.2005.00086.x

Wu, M., J. S. P. McCain, E. Rowland, R. Middag, A. E. Allen, and E. M. Bertrand. 2019. Manganese and iron deficiency in Southern Ocean *Phaeocystis antarctica* populations revealed through taxon-specific protein indicators. Nat. Commun. **1–10**: 3582. doi:10.1038/s41467-019-11426-z

Zhu, Z., K. Xu, F. Fu, J. L. Spackeen, D. A. Bronk, and D. A. Hutchins. 2016. A comparative study of iron and temperature interactive effects on diatoms and *Phaeocystis antarctica* from the Ross Sea, Antarctica. Mar. Ecol. Prog. Ser. **550**: 39–51. doi:10.3354/meps11732

Acknowledgments

The authors would like to thank the captain, crew, ASC technicians, and scientists on the R/VIB N. B. Palmer (NBP 14-09) for the valuable help and support. We would also like to thank John Butterfield, Erin Dillon, Caroline Ferguson, Ella Patterson, and Alessandra Santiago for help collecting samples, Marc Picheral for developing EcoTaxa for use with FlowCam images, and Elden Rowland for help with protein measurements. This research was funded by a grant from the National Science Foundation Office of Polar Programs to K.R.A. (ANT-1063592) and was developed under the STAR Fellowship Assistance agreement FP-91770101-1 awarded to H.J.W. by the U.S. Environmental Protection Agency (EPA; It has not been formally reviewed by EPA and views expressed are solely those of the authors). This research was also funded by an NSERC Discovery Grant RGPIN-2015-05009 and Simons Foundation Grant 504183 to E.M.B; Nova Scotia Graduate Scholarship to L.J.J.; Royal Netherlands Institute for Sea Research Ocean Systems Department funding to R.M.; and the University of Otago Doctoral Scholarship to K.S. Data presented in this paper are available in the Stanford Digital Depository: https://doi.org/10.25740/hd938dh1291.

Conflict of Interest

None declared.

Submitted 02 November 2020
Revised 14 January 2022
Accepted 16 January 2022

Associate editor: Susanne Menden-Deuer